

IHMTTC2015- 1450

IMPLEMENTATION OF KNUDSEN LAYER EFFECTS IN OPEN SOURCE CFD SOLVER FOR EFFECTIVE MODELING OF MICROSCALE GAS FLOWS

Shashank Jaiswal

Department of Mechanical and Aerospace Engineering
Indian Institute of Technology Hyderabad
Email: me12b1033@iith.ac.in

Nishanth Dongari

Department of Mechanical and Aerospace Engineering
Indian Institute of Technology Hyderabad
Email: nishanth@iith.ac.in

ABSTRACT

We incorporate the power law (PL) based geometry dependent mean free path (MFP) model into the open-source computational fluid dynamics (CFD) software OpenFOAM. As gas transport properties can be related to the mean free path through kinetic theory, the Navier-Stokes-Fourier constitutive relations are then modified in order to model the flow behavior in the Knudsen layers close to surfaces. The velocity slip and temperature jump boundary conditions are also modified in the rhoCentralFoam solver. We carry out numerical simulations in order to accurately capture the knudsen-layer effect in microscale gas flows. Our model implementation is validated against the direct simulation Monte-Carlo (DSMC) data. The modified rhoCentralFOAM solver is applied to low and high mach number velocity-driven (Couette) flow and Fourier heat transfer in microchannels. The results show that our solver greatly improves the near-wall accuracy of the Navier-Stokes-Fourier equations, well beyond the slip-flow regime. The importance of this paper stems from the numerical simulation point of view, as OpenFOAM tool is open source, parallel-friendly, and able to solve flows involving complex geometries and unstructured mesh.

Keywords: Microscale Gas Flows, Knudsen Layer, CFD, OpenFOAM, Slip Boundary Conditions

NOMENCLATURE

Kn	Knudsen Number
Pr	Prandtl Number
p	Pressure (Pa)
U	Velocity (m/s)
T	Temperature (K)
Ma	Mach number
H	Distance between parallel plates
m	Molecular mass (kg)
A_s	First Sutherland coefficient (kg/(s.m.K ^{1/2}))
T_s	Second Sutherland coefficient (K)
γ	Adiabatic index
λ	Gas mean free path
λ_{eff}	Effective gas mean free path
β_{PL}	Normalized mean free path
ρ	Density (kg/m ³)
μ	Viscosity (kg/ms)
ψ	Compressibility (s ² /m ²)
κ	Thermal conductivity (W/mK)
n	Boundary patch normal
α_h	Thermal diffusivity of enthalpy (kg/ms)
σ_v	Accommodation Coefficient : Velocity
σ_t	Accommodation Coefficient : Temperature

INTRODUCTION

In micro/rarefied gas flows, the gas molecule wall-surface interactions lead to the formation of Knudsen layer (KL): a local thermodynamically non-equilibrium region

extending $\sim O(\lambda)$ from the surface, where λ is the gas mean free path (MFP). Since the gas molecule-surface collisions are more frequent than gas molecule-molecule collisions in the KL, the gas MFP will effectively be reduced in the KL. It is noticed that the classical constitutive relations of the Navier-Stokes-Fourier (NSF) equations fail to predict non-linear behavior in the KL and deviations are significant in the slip and transition flow regimes [1]. Ideally, one can resort to carrying out DSMC [2] studies to provide accurate predictions in the KL region but they are computationally intensive for low-speed flows in the slip and transition-flow regime.

Alternatively, geometry dependent effective molecular mean free path [3–9] models are incorporated to extend the applicability of the Navier-Stokes-Fourier equations in the KL region. This phenomenological observation of the bounding wall effect on the NSF constitutive laws has been interpreted as the modification of the gas MFP due to gas molecule/wall surface collisions [10]. These approaches have produced good results when compared with DSMC and molecular-dynamics (MD) data for various rarefied gas flow problems [4, 5, 7–9].

The molecular dynamics (MD) simulations carried out by Dongari et al. [8] indicate that the free paths of gas molecules follow a power-law (PL) distribution. The author then accordingly hypothesized that the probability distribution function for the MFP of a rarefied gas followed a PL form, which is validated against MD data under various rarefied conditions. While the classical exponential MFP scaling models [5, 7] are limited up to $Kn \sim 0.2$, power-law based effective MFP models exhibit good agreement with the MD data up to the early transition regime ($Kn \sim 1$). Subsequently, the Navier-Stokes-Fourier constitutive relations and the slip and jump boundary conditions are modified using PL-based MFP scaling which accurately captured several non-equilibrium effects in the Knudsen layer.

We implement the power law based scaling approach as proposed by Dongari et al. [9] due to its applicability up to the early transition regime ($Kn \sim 1$). The implementation has been done in an open source CFD package OpenFOAM®. OpenFOAM [11, 12] is an open source CFD software package (based on C++ programming language [13]) which is capable of solving partial differential equations on unstructured meshes in parallel. The wall scaling model is incorporated in rhoCentralFoam solver by changing the library files of thermo-physical models, slip and jump boundary conditions. In this paper analysis of subsonic and transonic Couette flow, and Fourier heat

transfer between parallel plates have been carried out for various Kn values covering both slip and transition regimes.

NUMERICAL SIMULATIONS

The OpenFOAM [11, 12] (Open Field Operation and Manipulation) CFD Toolbox is a free, open source CFD software package which has an extensive range of features to solve complex fluid flow problems for arbitrary structured and unstructured grids. OpenFOAM is primarily written in the object oriented programming language C++ [13]. It makes heavy use of the concepts of C++ templates, function and operator overloading [11]. Almost everything (including meshing, and pre-processing and post-processing) runs in parallel as standard, enabling users to take full advantage of computer hardware. By being open source under the terms of GNU Public License (GPL), OpenFOAM offers its users the complete freedom to customize and extend its existing functionality.

rhoCentralFOAM [14] is a compressible solver available in OpenFOAM which has the capability to simulate arbitrary 2D and 3D geometries along with Dirichlet, Neumann or Robin boundary conditions. It employs the central scheme formulation as proposed by Kurganov and Tadmor [15, 16]. *rhoCentralFOAM* has been benchmarked [14] and have been widely used for studying hypersonic [17], subsonic [18] and thermal [19, 20] gas flow problems.

IMPLEMENTATION OF EFFECTIVE MFP

The geometry dependent effective MFP [4, 5, 7, 9] models have been incorporated to extend the applicability of the Navier-Stokes equations in the KL region. The viscosity correction models based on wall function corrections have been already proposed and well established [4, 5, 7, 9, 21, 22]. We incorporate the effective MFP expression developed by Dongari et al. [9] for planar geometries.

Parallel Plate Geometries

The power law (PL) based effective MFP can be expressed as :

$$\begin{aligned} \lambda_{\text{eff(PL)}} &= \frac{\lambda}{2} [p(r^-) + p(r^+)] \\ &= \lambda \left\{ 1 - \frac{1}{2} \left[\left(1 + \frac{r^-}{a} \right)^{1-n} + \left(1 + \frac{r^+}{a} \right)^{1-n} \right] \right\} \end{aligned} \quad (1)$$

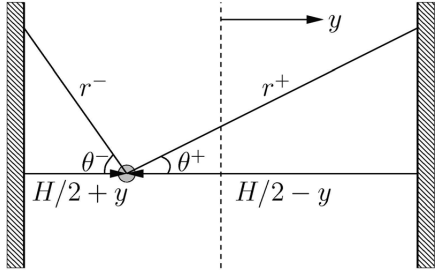


FIGURE 1. A molecule confined between two planar walls with spacing H . The molecule has an equal probability to travel in any zenith angle θ^- or θ^+ or to travel in either the positive or negative y direction. The molecule under consideration is assumed to have just experienced an intermolecular collision at its current position $H/2 + y$.

where λ is unconfined gas mean free path, $p(r)$ is the power-law probability distribution function, $a = \lambda(n - 2)$ and $n = 3$ unless otherwise explicitly stated.

A three-dimensional MFP can be obtained by averaging the free path with respect to θ^- and θ^+ in the range $[0, \pi/2]$ using the mean integral theorem as :

$$\langle \lambda_{\text{eff(PL)}}(\theta) \rangle = \frac{2}{\pi} \int_0^{\pi/2} \lambda_{\text{eff(PL)}}(\theta) d\theta \quad (2)$$

which upon averaging over free path using Simpson's numerical integration over 16 subintervals results in $\lambda_{\text{eff}} = \lambda \beta_{\text{PL}}$, where

$$\begin{aligned} \beta_{\text{PL}} = 1 - \frac{1}{96} & \left[\left(1 + \frac{H/2 - y}{a}\right)^{1-n} + \left(1 + \frac{H/2 + y}{a}\right)^{1-n} \right. \\ & + 4 \sum_{i=1}^8 \left(1 + \frac{H/2 - y}{a \cos[(2i-1)\pi/32]}\right)^{1-n} \\ & + 4 \sum_{i=1}^8 \left(1 + \frac{H/2 + y}{a \cos[(2i-1)\pi/32]}\right)^{1-n} \\ & + 2 \sum_{i=1}^7 \left(1 + \frac{H/2 - y}{a \cos[i\pi/16]}\right)^{1-n} \\ & \left. + 2 \sum_{i=1}^7 \left(1 + \frac{H/2 + y}{a \cos[i\pi/16]}\right)^{1-n} \right] \quad (3) \end{aligned}$$

We use the effective viscosity model which can be ex-

pressed as :

$$\mu_{\text{eff}} = \mu \beta_{\text{PL}} \quad (4)$$

where μ is Sutherland's temperature dependent viscosity and given below,

$$\mu = \frac{A_s \sqrt{T}}{1 + T_s/T} \quad (5)$$

Therefore effective viscosity can be expressed as:

$$\mu_{\text{eff}} = \beta_{\text{PL}} \frac{A_s \sqrt{T}}{1 + T_s/T} \quad (6)$$

The unconfined MFP for energy transfer between molecules can be defined as $\lambda_t = 1.922 \lambda_{\text{HS}}$, where the subscript HS denotes hard-sphere molecules [1, 9]. Therefore, the modified constant for thermal cases becomes :

$$a_t = \lambda_t (n - 2) \quad (7)$$

Further, the normalized effective MFP for thermal Knudsen layer can be defined as $(\beta_{\text{PL}})_t$, which can be obtained by replacing a with a_t in Eq. (3).

Thermal conductivity (κ) is calculated using viscosity (μ). Thermal diffusivity of enthalpy (α_h) is calculated using thermal conductivity (κ). With a change in original viscosity to effective viscosity, these quantities have also been modified accordingly.

Since μ is a scalar field defined on cell-centers of collocated mesh, the correction i.e., β_{PL} is also defined as a scalar field on cell-centers of collocated mesh. For the purpose of calculating β_{PL} in a particular cell, we take the cell centre coordinate of the cell and find its wall normal distance corresponding to the two walls which is then substituted in the equation (3). Since the equation is symmetric, the order in which we substitute the wall normal distance values does not matter. As far as β_{PL} values at zero-volume boundary patches is concerned, we take face-center coordinate values and proceed with our calculation. The original rhoCentralFoam solver implements the Sutherland's viscosity model. We modify the Sutherland's viscosity model by multiplying the original viscosity with β_{PL} over the entire domain. The other properties such as α ,

κ has to be subsequently modified.

The modified Navier-Stokes constitutive relation also needs to be solved in conjunction with appropriate slip boundary condition to capture the non-equilibrium phenomena in the KL [9].

OpenFOAM implements the Maxwell velocity slip and Smolouchowski temperature jump boundary conditions in rhoCentralFoam solver. The current implementation of Maxwell velocity slip and Smolouchowski temperature jump in OpenFOAM can be mathematically expressed as [14, 19, 23]:

$$U + \frac{2 - \sigma_v}{\sigma_v} \lambda \nabla_n(S.U) = U_{wall} - \frac{2 - \sigma_v}{\sigma_v} \frac{\lambda}{\mu} S.(n.\Pi_{mc}) - \frac{3}{4} \frac{\mu}{\rho} \frac{S.\nabla T}{T} \quad (8)$$

$$T = T_{wall} - \frac{2 - \sigma_t}{\sigma_t} \frac{2\gamma}{(\gamma + 1)Pr} \lambda (n.\nabla T) \quad (9)$$

respectively, with,

$$\frac{\lambda}{\mu} = \sqrt{\frac{\pi\psi}{2}} \frac{1}{\rho} \quad (10)$$

$$\Pi_{mc} = \mu(\nabla U)^T - (2/3)Itr(\nabla U) \quad (11)$$

where $S = I - nn$ is the identity tensor which removes normal components of any nonscalar field, eg. velocity, so that slip occurs in the direction tangential to surface. Three terms that appear on right side of equation (8) equation correspond to wall velocity, curvature effect and thermal creep respectively.

For our planar geometry, effect of the curvature is negligible. Hence, equation (8) using (10) can be simplified to:

$$U = U_w - \frac{2 - \sigma_v}{\sigma_v} \sqrt{\frac{\pi\psi}{2}} \frac{\mu}{\rho} \nabla_n(S.U) - \frac{3}{4} \frac{\mu}{\rho} \frac{S.\nabla T}{T} \quad (12)$$

which for our implementation acquires the following form:

$$U = U_w - \frac{2 - \sigma_v}{\sigma_v} \sqrt{\frac{\pi\psi}{2}} \frac{\mu \beta_{PL}}{\rho} \nabla_n(S.U) - \frac{3}{4} \frac{\mu (\beta_{PL})_T}{\rho} \frac{S.\nabla T}{T} \quad (13)$$

Smolouchowski temperature jump equation (9) using (10) can be expressed as:

$$T = T_w - \frac{2 - \sigma_t}{\sigma_t} \frac{2\gamma}{(\gamma + 1)Pr} \sqrt{\frac{\pi\psi}{2}} \frac{\mu}{\rho} (n.\nabla T) \quad (14)$$

which for our implementation acquires the following form:

$$T = T_w - \frac{2 - \sigma_t}{\sigma_t} \frac{2\gamma}{(\gamma + 1)Pr} \sqrt{\frac{\pi\psi}{2}} \frac{\mu (\beta_{PL})_T}{\rho} (n.\nabla T) \quad (15)$$

TEST CASES

The comparisons have been made with the multiple results of dsmc simulations [24–26] for verifying the validity of our implemented model. For all the test cases involving parallel plate geometry, the Knudsen number is given by $Kn = \lambda/H$, the accommodation coefficients σ_t & σ_v are assigned a value of unity; i.e. fully diffuse reflection has been assumed for both walls. The first-order velocity-slip (Maxwell Slip) and temperature-jump (Smolouchowski Jump) boundary conditions for the NSF equations have been applied at walls. The viscosity was obtained from Sutherland's law. Sutherland's coefficients for argon are $R = 208 J/(kg.K)$, $T_s = 144 K$ and $A_s = 1.96e-6 kg/(s.m.K^{1/2})$ [24]. Unless otherwise explicitly stated, these conditions remain the same.

Subsonic Couette Flow

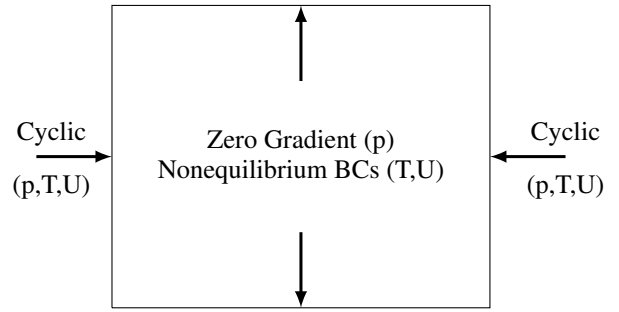


FIGURE 2. Numerical setup for Couette flow case

For this test case, the coordinates are chosen such that the walls are parallel to the x-direction and y is the direction perpendicular to the plates. The two parallel plates have been set at $y = \pm H/2$. The upper and lower plates move with a constant velocity $U_w = \pm 50$

ms^{-1} , in opposite directions, and the external acceleration $a_x = a_y = 0$. The wall temperature is fixed at $T_w = 273$ K.

In the Fig. 3, the cross sectional normalized velocity profiles obtained from the KL model (implemented in OpenFOAM) have been compared with the DSMC data and the classical slip model for $Kn=0.5$ and $Kn=1.0$ [24]. At $Kn=0.50$ and $Kn=1.0$, the conventional NS equations with maxwell slip boundary condition significantly under-predicts the velocity in the near-wall region. Our Knudsen layer model is in fair agreement with the DSMC solution, although it slightly under-predicts the maximum velocity (which is negligible when compared with the conventional slip model solution).

The conventional NSF equations with the non-equilibrium boundary conditions cannot account for the non-linear flow behaviour observed in Knudsen-layer [1, 3, 9, 27]. With increase in Kn , the wall-scale dependence of MFP is more pronounced, which significantly affects the thickness of Knudsen layer. The NSF equations get affected due to the modification in transport properties (for example: μ , κ which play an important role in non-equilibrium gas flows [2]). The deviation between *conventional slip model* and *knudsen layer model* with Knudsen number can be attributed to this modification [8, 9].

Transonic Couette Flow

For this test case, the coordinates are chosen such that the walls are parallel to the x-direction and y is the direction perpendicular to the plates. The two parallel plates have been set at $y = 0$ and $y=H$. The upper remains stationary while the lower wall moves with a constant velocity of \sqrt{RT} , and the external acceleration $a_x = a_y = 0$. The wall temperature is fixed at $T_w = 273$ K.

In the Fig. 4, the cross sectional normalized velocity profiles obtained from the KL model (implemented in OpenFOAM) have been compared with the DSMC data and the classical slip model for $Kn=0.5$ and $Kn=1.0$ [25]. At $Kn=0.50$ and $Kn=1.00$, the conventional NS equations with maxwell slip boundary condition significantly under-predicts the velocity in the near-wall region. Our Knudsen layer model is in excellent agreement with the DSMC solution with minor deviations in predicted maximum velocity.

Fourier Heat Transfer

Earlier test cases dealt with velocity driven flows, where we have demonstrated the accuracy of Knudsen layer modeling of momentum equations. Here, we showcase the

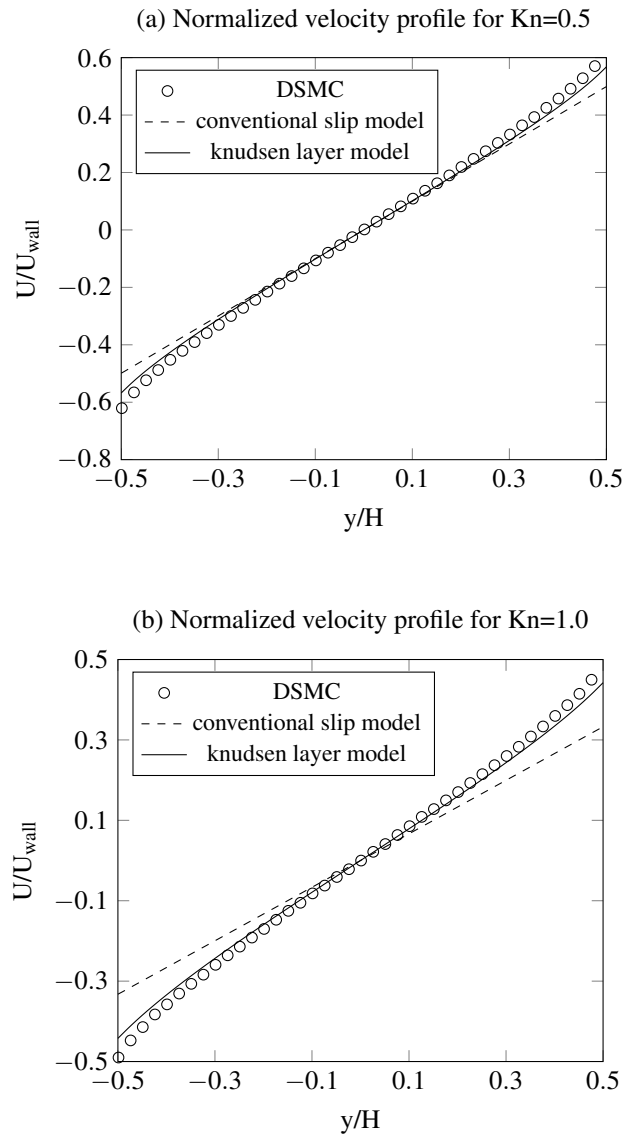


FIGURE 3. Normalized velocity profiles in subsonic micro-channel Couette flow under rarefied conditions. (a) $Kn=0.5$ and (b) $Kn=1.0$. Here Knudsen layer model results are compared against DSMC data [24] and the conventional slip model.

accuracy of thermal Knudsen layer modeling of energy equation by solving the Fourier heat transfer problem. For this test case, the geometrical setup is same as in case of Transonic Couette Flow. The upper and lower walls remain stationary. The lower wall i.e, cold junction temperature is fixed at $T_w = 263$ K while the upper wall i.e, hot junction temperature is fixed at 283K.

In the Fig. 5, the cross sectional normalized velocity

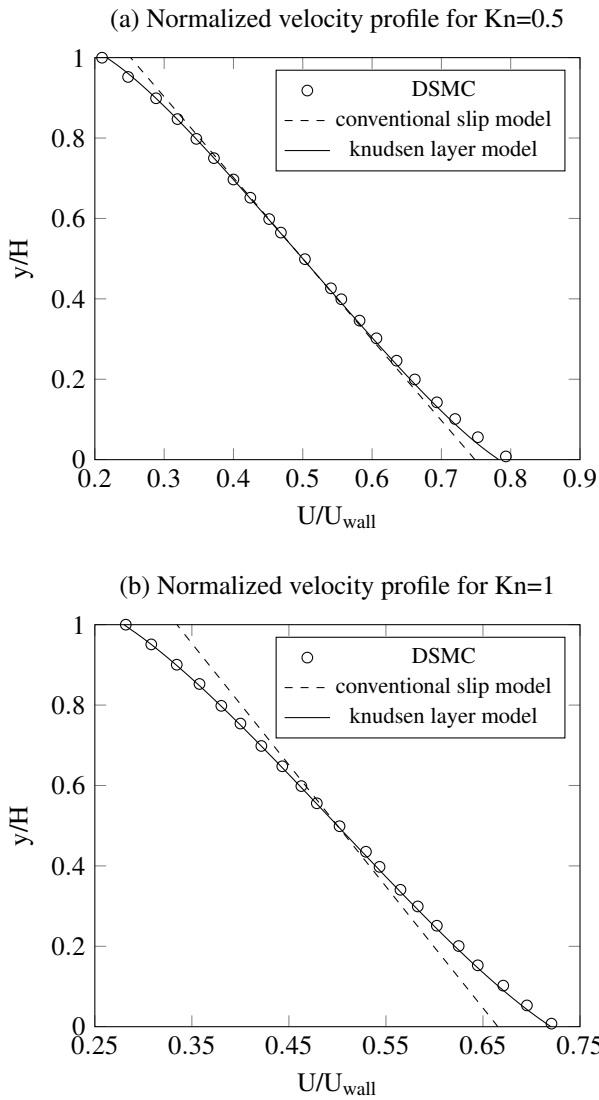


FIGURE 4. Normalized velocity profiles in transonic micro-channel Couette flow under rarefied conditions. (a) $Kn=0.5$ and (b) $Kn=1.0$. Here Knudsen layer model results are compared against DSMC data [25] and the conventional slip model.

profiles obtained from the KL model (implemented in OpenFOAM) have been compared with the DSMC data and the classical slip model for $Kn=0.475$ and $Kn=1.58$ [26]. For both Knudsen numbers 0.475 and 1.58, the conventional NS equations significantly under-predicts the velocity in the near region. Our Knudsen layer model is in fair agreement with the DSMC solution, although minor deviations are noticed in the near-wall (which is negligible when compared with the conventional slip model solution).

With a change in Knudsen number, momentum equa-

tions as well as energy equations gets modified. The variation in results is attributed to modification of MFP, which affects transport properties [9].

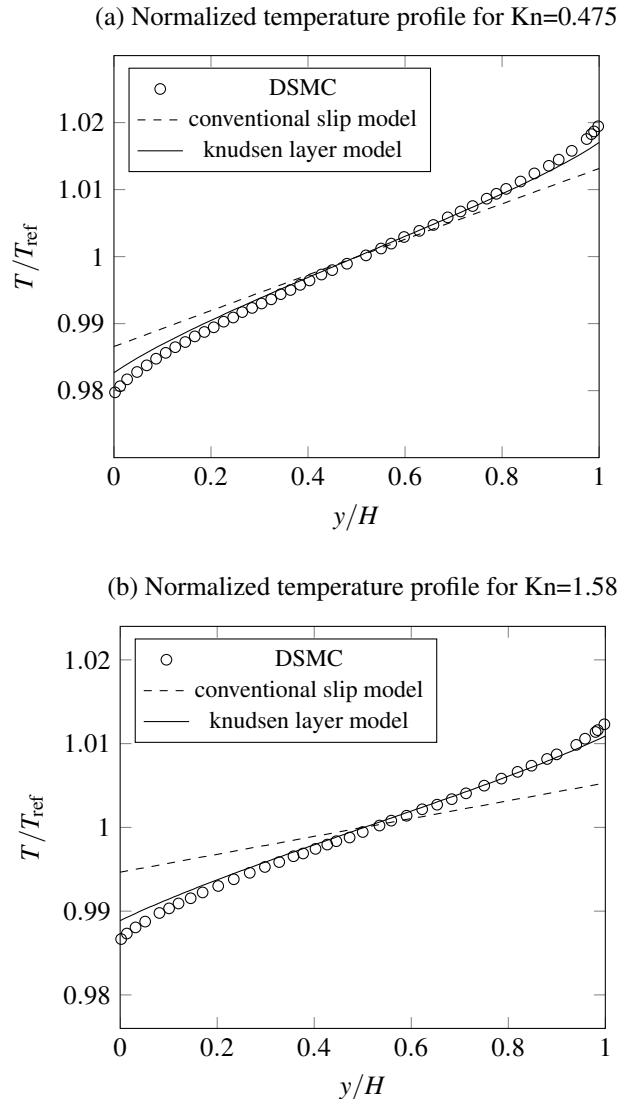


FIGURE 5. Normalized temperature profiles in micro-channel Fourier heat transfer under rarefied conditions. (a) $Kn=0.475$ and (b) $Kn=1.58$. Here Knudsen layer model results are compared against DSMC data [26] and the conventional slip model.

CONCLUSIONS

We have implemented the power-law based constitutive scaling approach to model the Knudsen layer flow within a

conventional continuum fluid dynamics framework OpenFOAM. This implementation has been tested for the cases of subsonic and transonic Couette gas flows and Fourier heat transfer in microchannels.

In general, the implementation is more accurate than the conventional model in capturing many non-equilibrium effects in the transition regime. Our results for the subsonic and transonic Couette gas flows as well as Fourier heat transfer in micro/nanochannels indicate that it provides a reasonable description of the nonlinear flow characteristics in the Knudsen layer up to $\text{Kn} \sim O(\lambda)$.

While it is important not to draw strong conclusions based on just three test cases, the present results may motivate future work into understanding the origin of non-equilibrium physics in rarefied gases, including:

1. whether the power-law behavior is appropriate for rarefied gases in complex geometries
2. effectiveness of above model in capturing the specular-diffusive and rough walls effects.
3. revisiting higher-order velocity slip and temperature jump boundary conditions.

REFERENCES

- [1] Sone, Y., 2002. *Kinetic theory and fluid dynamics*. Springer Science & Business Media.
- [2] Bird, G. A., 1994. “Molecular gas dynamics and the direct simulation of gas flows”.
- [3] Cercignani, C., 1988. *The Boltzmann equation*. Springer.
- [4] Guo, Z., Shi, B., and Zheng, C. G., 2007. “An extended navier-stokes formulation for gas flows in the knudsen layer near a wall”. *Europhysics Letters*, **80**(2), p. 24001.
- [5] Stops, D., 1970. “The mean free path of gas molecules in the transition regime”. *Journal of Physics D: Applied Physics*, **3**(5), p. 685.
- [6] Lockerby, D. A., and Reese, J. M., 2008. “On the modelling of isothermal gas flows at the microscale”. *Journal of Fluid Mechanics*, **604**, pp. 235–261.
- [7] Arlemark, E. J., Dadzie, S. K., and Reese, J. M., 2010. “An extension to the navier–stokes equations to incorporate gas molecular collisions with boundaries”. *Journal of Heat Transfer*, **132**(4), p. 041006.
- [8] Dongari, N., Zhang, Y., and Reese, J. M., 2011. “Molecular free path distribution in rarefied gases”. *Journal of Physics D: Applied Physics*, **44**(12), p. 125502.
- [9] Dongari, N., Zhang, Y., and Reese, J. M., 2011. “Modeling of knudsen layer effects in micro/nanoscale gas flows”. *Journal of Fluids Engineering*, **133**(7), p. 071101.
- [10] Zhang, Y.-H., Gu, X.-J., Barber, R. W., and Emerson, D. R., 2006. “Capturing knudsen layer phenomena using a lattice boltzmann model”. *Physical Review E*, **74**(4), p. 046704.
- [11] Weller, H. G., Tabor, G., Jasak, H., and Fureby, C., 1998. “A tensorial approach to computational continuum mechanics using object-oriented techniques”. *Computers in physics*, **12**(6), pp. 620–631.
- [12] Jasak, H., Jemcov, A., and Tukovic, Z., 2013. “Openfoam: A c++ library for complex physics simulations”.
- [13] Stroustrup, B., 1986. *The C++ programming language*. Pearson Education India.
- [14] Greenshields, C. J., Weller, H. G., Gasparini, L., and Reese, J. M., 2010. “Implementation of semi-discrete, non-staggered central schemes in a colocated, polyhedral, finite volume framework, for high-speed viscous flows”. *International journal for numerical methods in fluids*, **63**(1), pp. 1–21.
- [15] Kurganov, A., and Tadmor, E., 2000. “New high-resolution central schemes for nonlinear conservation laws and convection–diffusion equations”. *Journal of Computational Physics*, **160**(1), pp. 241–282.
- [16] Kurganov, A., Noelle, S., and Petrova, G., 2001. “Semidiscrete central-upwind schemes for hyperbolic conservation laws and hamilton–jacobi equations”. *SIAM Journal on Scientific Computing*, **23**(3), pp. 707–740.
- [17] Greenshields, C. J., and Reese, J. M., 2012. “Rarefied hypersonic flow simulations using the navier–stokes equations with non-equilibrium boundary conditions”. *Progress in Aerospace Sciences*, **52**, pp. 80–87.
- [18] Bohorquez, P., and Parras, L., 2013. “Three-dimensional numerical simulation of the wake flow of an afterbody at subsonic speeds”. *Theoretical and Computational Fluid Dynamics*, **27**(1-2), pp. 201–218.
- [19] Mohammadzadeh, A., Roohi, E., Niazmand, H., Stefanov, S., and Myong, R. S., 2012. “Thermal and second-law analysis of a micro-or nanocavity using direct-simulation monte carlo”. *Physical Review E*, **85**(5), p. 056310.
- [20] Le, N. T., White, C., Reese, J. M., and Myong, R. S., 2012. “Langmuir–maxwell and langmuir–smoluchowski boundary conditions for thermal gas flow simulations in hypersonic aerodynamics”. *International Journal of Heat and Mass Transfer*, **55**(19), pp. 5032–5043.
- [21] Lockerby, D. A., Reese, J. M., and Gallis, M. A., 2005. “Capturing the knudsen layer in continuum-fluid mod-

- els of nonequilibrium gas flows”. *AIAA journal*, **43**(6), pp. 1391–1393.
- [22] Fichman, M., and Hetsroni, G., 2005. “Viscosity and slip velocity in gas flow in microchannels”. *Physics of Fluids (1994-present)*, **17**(12), p. 123102.
- [23] Le, N., Greenshields, C. J., and Reese, J., 2012. “Evaluation of nonequilibrium boundary conditions for hypersonic rarefied gas flows”. In *Progress in Flight Physics*, Vol. 3, EDP Sciences, pp. 217–230.
- [24] Gu, X.-j., and Emerson, D. R., 2009. “A high-order moment approach for capturing non-equilibrium phenomena in the transition regime”. *Journal of Fluid Mechanics*, **636**, pp. 177–216.
- [25] Xue, H., and Ji, H., 2003. “Prediction of flow and heat transfer characteristics in micro-couette flow”. *Microscale Thermophysical Engineering*, **7**(1), pp. 51–68.
- [26] Gallis, M., Rader, D., and Torczynski, J., 2002. “Calculations of the near-wall thermophoretic force in rarefied gas flow”. *Physics of Fluids (1994-present)*, **14**(12), pp. 4290–4301.
- [27] Chen, S., and Doolen, G. D., 1998. “Lattice boltzmann method for fluid flows”. *Annual review of fluid mechanics*, **30**(1), pp. 329–364.